Physics of the Solid State, 2024, Vol. 66, No. 11

13,12

# Reorientational motion of cobaltocene intercalated into titanium diselenide: NMR study

© A.V. Soloninin, A.V. Skripov, A.N. Titov

M.N. Mikheev Institute of Metal Physics, Ural Branch, Russian Academy of Sciences,
Yekaterinburg, Russia

E-mail: alex.soloninin@imp.uran.ru

Received August 20, 2024
Revised October 22, 2024
Accepted November 4, 2024

To study the dynamics of cobaltocene molecules $\mathrm{Co}(\pi-\mathrm{C_5H_5})_2$ intercalated into quasi-two-dimensional titanium diselenide $\mathrm{TiSe_2}$, we have measured the proton spin-lattice relaxation times and $^1$H nuclear magnetic resonance (NMR) spectra in $\mathrm{TiSe_2}\left(\mathrm{Co}(\pi-\mathrm{C_5H_5})_2\right)_{1/4}$ compound over the temperature range of 5−360 K. The existence of two types of reorientational motion of $\mathrm{Co}(\pi-(\mathrm{C_5H_5})_2)$ molecules has been found. The faster reorientational process related to rotations of $\mathrm{C_5H_5}$ rings around the 5-fold symmetry axis is characterized by the activation energy of 60 meV, and the slower process determined by reorientations of cobaltocene molecules around the 2-fold symmetry axis is characterized by the activation energy of 155 meV. Measurements of $^1$H NMR parameters in molecular cobaltocene have shown that for this compound the dominant mechanism of the proton spin-lattice relaxation is determined not by motion of $\mathrm{Co}\left(\pi-(\mathrm{C_5H_5})_2\right)$ molecules, but by fluctuations of the localized electronic magnetic moment on cobalt.

**Keywords:** metallocenes, transition-metal dichalcogenides, intercalation, spin-lattice relaxation, reorientations.

DOI: 10.61011/PSS.2024.11.60110.219

## 1. Introduction

The discovery of metallocenes $M(\mathrm{C_5H_5})_2$, where $M$ is a metal atom [1], served as an impetus for the study of the atomic and electronic structure of this class of compounds. Metallocenes formed by various $3d$-transition metals and $\mathrm{C_5H_5}$ ring ligand are found to be isomorphic at room temperature and have a similar crystal structure [2–4]. Figure 1 shows a cobaltocene molecule and the monoclinic structure of a molecular crystal of $\mathrm{Co}(\pi-\mathrm{C_5H_5})_2$.

The electronic structure of metallocenes of $3d$-transition metals is well described within the framework of the molecular orbital method in the approximation of a linear combination of atomic orbitals (MO LCAO) [5], and also within the framework of density functional theory (DFT) [6]. An unpaired electron in the antibonding orbital of crystalline colbatocene creates a magnetic moment equal to 1.76 Bohr mageton, and measurements of magnetic susceptibility at low temperature (from 4.2 to 77 K) have demonstrated the presence of weak antiferromagnetic ordering [7]. Studies of the heat capacity of cobaltocene have revealed a feature in the temperature range of 70−120 K with a maximum at 93.5 K, which is attributable to a phase transition associated with the orientational ordering of $\mathrm{C_5H_5}$ rings [8]. X-ray diffraction examination of cobaltocene at room temperature revealed two types of mutual orientation of $\mathrm{C_5H_5}$ rings (antiprismatic conformation with reorientation disorder and prismatic conformation); the orientational ordering of the rings takes place in the prismatic conformation when the temperature decreases [8,9].

The first studies related to the intercalation of metallocene molecules into layered disulfides and diselenides of transition metals were published in Ref. [10]. Currently, interest in intercalated layered chalcogenides has increased due to the special properties of these materials with reduced dimensionality, which can be used for a number of applications, including energy storage (batteries, capacitors), catalysis, superconductivity, etc. [11–14]. X-ray and neutron diffraction methods have shown that intercalation of chalcogenides with cobaltocene results in an increase of the distance between the chalcogen−metal−chalcogen layers and cobaltocene molecules are arranged so that their fifth-order symmetry axis $C_5$ is parallel or perpendicular to these layers [15–18]. Intercalation of cobaltocene into chalcogenides results in the ionization of cobaltocene, $\mathrm{Co(C_5H_5)_{2+}}$. Theoretical studies of the possible orientations of cobaltocene molecules in $\mathrm{SnS_2}$ and $\mathrm{SnSe_2}$ dichalcogenides have shown that the orientation of the axis $C_5$ parallel to the dichalcogenide layers is energetically favourable [19,20].

The nuclear magnetic resonance (NMR) method is an effective method for studying molecular dynamics in solids at the microscopic level [21]. Currently, there are few studies of metallocene mobility in dichalcogenides by the NMR method. For example, the molecular dynamics of cobaltocene intercalated into tantalum disulfide $\mathrm{TaS_2}$ was studied in Ref. [22]. The temperature dependences of the shape of $^1$H NMR lines and the second moments of these lines have been studied using the wide-line NMR method. The parameters of the reorientation of

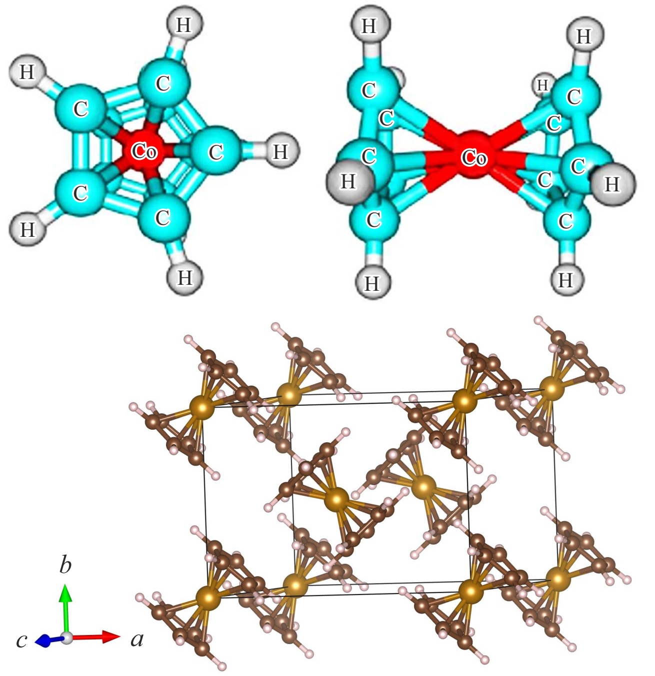

**Figure 1.** Schematic view of the cobaltocene molecule (in two projections) and the monoclinic structure of $Co(\pi-C_5H_5)_2$ molecular crystal.

cobaltocene molecules were determined based on these experimental data and a model was proposed describing the possible location of these molecules between the tantalum disulfide layers. Ref. [22] assumes that at low temperatures cobaltocene molecules rotate around the fifth-order symmetry axis, which is parallel to the dichalcogenide layers, and reorientation around the second-order symmetry axis is also excited with the increase of the temperature. Recording of NMR spectra on the deuterium nucleus, $^2H$, in dichalcogenides intercalated with cobaltocene also shows that the reorientation of cobaltocene molecules is possible around the symmetry axes of the second and fifth orders [23–26].

Magnetic susceptibility and electrical resistance were studied as a function of temperature in synthesized titanium diselenide [27] intercalated with cobaltocene, $TiSe_2(Co(\pi-C_5H_5)_2)_{1/4}$ [28]. It is shown that the observed paramagnetic Curie temperature was zero for $TiSe_2(Co(\pi-C_5H_5)_2)_{1/4}$, which indicates the absence of magnetic interaction in the material. The deviation from the paramagnetic dependence in the temperature range below 10 K was attributed to a change of the charge state of cobalt, but not to the magnetic ordering [28]. It was found that the electrical resistance of $TiSe_2(Co(\pi-C_5H_5)_2)_{1/4}$ organometallic compound decreases by eight orders of magnitude when a pressure of 20 GPa is applied [29,30]. Cobaltocene intercalated into titanium diselenide can be considered as a pseudo-alkali metal [10], which also transfers an electron to chalcogenide, and therefore these materials can be studied as objects for energy storage. The atomic motion of $C_5H_5$ ligands in titanium diselenide intercalated with cobaltocene has not been studied so far. Experimental data on the dynamics of cobaltocene rings obtained by $^1H$ NMR in wide frequency and temperature ranges will be presented in this paper.

## 2. Experiment

The preparation of samples of $Co(\pi-C_5H_5)_2$ and $TiSe_2(Co(\pi-C_5H_5)_2)_{1/4}$ has been described in detail in Ref. [27,28]. The molecular crystal of cobaltocene has a monoclinic structure with lattice parameters $a = 5.926(4)$ Å, $b = 7.732(6)$ Å, $c = 10.618(8)$ Å, $\beta = 121.38(11)^\circ$, $V = 415.4$ Å$^3$ and with C–C average distances equal to 1.41(1) Å, and Co–C average distances equal to 2.096(8) Å [3]. Titanium diselenide has a hexagonal structure with lattice parameters $a = 3.540(3)$ Å, $c = 6.008(2)$ Å, and intercalation with cobaltocene increases the lattice constant $c$ by 5.693 Å [27,28]. The location of cobaltocene between the layers of titanium diselenide is shown in Figure 2. Cobaltocene occupies 1/4 of the possible octahedral positions in $TiSe_2$ interlayer space and forms $TiSe_2(Co(\pi-C_5H_5)_2)_{1/4}$ compound [28].

The spin-lattice relaxation time, $T_1$, was measured on $^1H$ nuclei using an upgraded SXP 4–100 NMR pulse spectrometer manufactured by „Bruker“ at frequencies of $\omega/2\pi = 14.5$, 23.8 and 90 MHz in the temperature range of 5–360 K. A two-pulse sequence $90^\circ-\tau-90^\circ$ with a variable interval $\tau$ between two 90° radio-frequency pulses

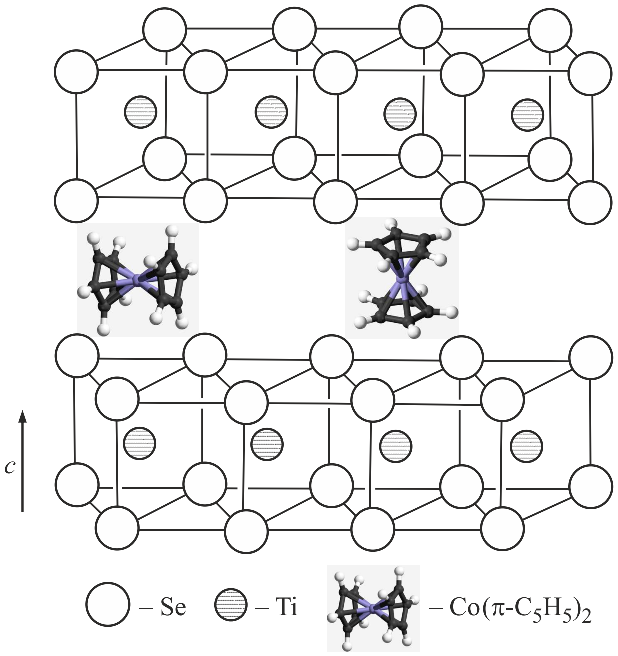

**Figure 2.** Diagram of the location of intercalated cobaltocene in titanium diselenide. The parallel and perpendicular orientation of the cobaltocene molecule in a layered lattice of $TiSe_2$ is shown.

was used to measure $T_1$. The relaxation of the nuclear magnetization of the studied compounds, $\mathrm{Co(\pi{-}C_5H_5)_2}$ and $\mathrm{TiSe_2\big(Co(\pi{-}C_5H_5)_2\big)_{1/4}}$, was described by a single-exponential function. The shape of $^1$H NMR line was recorded in the field $B_0 = 0.559\,\mathrm{T}$ using the Fourier transform of the solid echo signal. The spectra were recorded by magnetic field sweeping in the temperature range of 5–40 K, in which $^1$H NMR line width in $\mathrm{Co(\pi{-}C_5H_5)_2}$ exceeded 50 kHz. $\mathrm{Co(\pi{-}C_5H_5)_2}$ and $\mathrm{TiSe_2\big(Co(\pi{-}C_5H_5)_2\big)_{1/4}}$ were studied in sealed ampoules to avoid oxidation and destruction of the sample. The temperature in the cryostat was changed and stabilized using an ITC-4 temperature controller („Oxford Instruments"), and the temperature remained stable in the entire studied range with an accuracy of $\pm 0.1\,\mathrm{K}$.

## 3. Experimental results and their discussion

The results of measurements of the spin-lattice relaxation rate $T_1^{-1}$ for $^1$H nuclei in $\mathrm{TiSe_2\big(Co(\pi{-}C_5H_5)_2\big)_{1/4}}$ are presented in Figure 3.

Figure 3 shows that the relaxation rate exhibits two maxima: in the low-temperature range $\sim 100\,\mathrm{K}$, and in the room temperature range. These maxima strongly depend on the resonance frequency: the maxima $T_1^{-1}(T)$ shift towards high temperatures and their amplitude decreases, as the frequency increases. This behavior of $T_1^{-1}(T)$ can be attributed to the motion of cobaltocene molecules located in the interlayer space of titanium diselenide. The spin-lattice relaxation rate of $^1$H for this system can be defined as the sum of two contributions: the contribution associated with the presence of paramagnetic impurities $T_{1p}^{-1}$, the value of which can be estimated in the maximum field at low temperature, and the contribution associated with the internuclear dipole-dipole interaction, $T_{1d}^{-1}$, modulated by the motion of molecules containing hydrogen atoms. The analysis of experimental spin-lattice relaxation time data obtained at different resonance frequencies makes it possible to determine the motion parameters of cobaltocene molecules. The contribution associated with the motion of cobaltocene molecules, $T_{1d}^{-1}$, was obtained by subtracting $T_{1p}^{-1}$ from the observed relaxation rate. The value of $T_{1p}^{-1}$ estimated from experimental data at a frequency of 90 MHz at $T = 10\,\mathrm{K}$ and is equal to $0.686\,\mathrm{s}^{-1}$. $T_1^{-1}(T)$ experimental data, shown in Figure 3, suggest that two types of motion occur for cobaltocene intercalated into titanium diselenide: the relaxation rate maximum at low temperature can be attributed to the rotation of $\mathrm{C_5H_5}$ rings around the fifth-order axis, and $T_{1d}^{-1}$ maximum at high temperature can be attributed to rotations of the cobaltocene molecule around the second-order axis. This assumption correlates with Ref. [22], which notes that cobaltocene intercalated in tantalum disulfide can perform two types of motion.

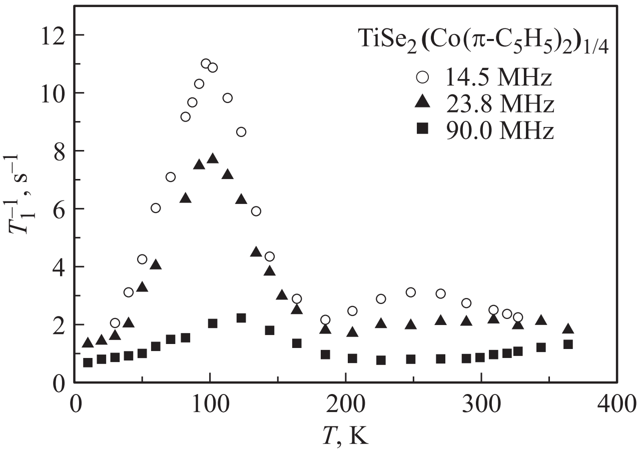

**Figure 3.** Temperature dependences of the proton spin-lattice relaxation rate in $\mathrm{TiSe_2\big(Co(\pi{-}C_5H_5)_2\big)_{1/4}}$ at three resonance frequencies.

The temperature dependence of the contribution of $T_{1d}^{-1}$ is characterized by a frequency-dependent maximum observed at a temperature at which the condition $\omega\tau_d \approx 1$ is fulfilled, where $\tau_d$ is the time between successive jumps of hydrogen atoms. First of all, let us consider the frequency-dependent peaks of the relaxation rate observed at low temperature. Figure 4 shows the dependence of $T_{1d}^{-1}$ on the inverse temperature for $\mathrm{TiSe_2\big(Co(\pi{-}C_5H_5)_2\big)_{1/4}}$ in the region of the low-temperature peak of the relaxation rate at frequencies of 90, 23.8 and 14.5 MHz.

$T_{1d}^{-1}(T)$ experimental results for molecular motion can be described by the standard model [31]. The dipole-dipole contribution to the proton spin-lattice relaxation rate in $\mathrm{TiSe_2\big(Co(\pi{-}C_5H_5)_2\big)_{1/4}}$ compound is determined in this model by $^1$H–$^1$H, $^1$H–$^{59}$Co interactions and is written as

$$\begin{aligned} T_{1d}^{-1} &= (T_{1d}^{-1})_{\mathrm{HH}} + (T_{1d}^{-1})_{\mathrm{HCo}} \\ &= \frac{2M_{2\mathrm{HH}}}{3\omega}\left[\frac{z}{1+z^2} + \frac{4z}{1+4z^2}\right] \\ &\quad + \frac{M_{2\mathrm{HCo}}}{2\omega}\left[\frac{z}{1+(1-b)^2z^2} + \frac{3z}{1+z^2} + \frac{6z}{1+(1+b)^2z^2}\right]. \end{aligned} \tag{1}$$

Here $z = \omega\tau_d$, $M_{2\mathrm{HH}}$ and $M_{2\mathrm{HCo}}$ are contributions to the second moment of $^1$H NMR line due to corresponding dipole-dipole interactions that fluctuate in the course of reorientational motion, $b = \gamma_{\mathrm{Co}}/\gamma_{\mathrm{H}}$, where $\gamma_{\mathrm{H}}$ and $\gamma_{\mathrm{Co}}$ are the gyromagnetic ratios for $^1$H and $^{59}$Co nuclei, respectively. Estimates of the second moments show that contributions from dipole-dipole interactions with other nuclei (including $^{77}$Se nuclei with a natural abundance of about 7.6%) can be ignored.

As follows from equation (1), the value of $T_{1d}^{-1}$ is proportional to $\tau_d$ in the limit of fast molecular motion ($z \ll 1$), and the value of $T_{1d}^{-1}$ is proportional to $\omega^{-2}\tau_d^{-1}$ in the limit of slow molecular motion ($z \gg 1$). If the temperature dependence $\tau_d$ is described by the Arrhenius law,

$$\tau_d = \tau_{d0} \exp\big(E_a/(k_\mathrm{B}T)\big), \tag{2}$$

where $E_a$ is the activation energy for motion, and $k_\mathrm{B}$ is the Boltzmann constant, we can expect that the graph of the dependence of $\ln T_{1d}^{-1}$ on $T^{-1}$ will be linear both in the limits of fast and slow motion with a slope determined by $E_a/k_\mathrm{B}$ and $-E_a/k_\mathrm{B}$, respectively. Deviations from the predictions of the standard model are observed in the experimental data shown in Figure 4. Firstly, the slope of the low-temperature branch of the dependence $\ln T_{1d}^{-1}$ on $T^{-1}$ turns out to be less than the slope of the high-temperature branch. Secondly, the observed frequency dependence of $T_{1d}^{-1}$ in the low-temperature region is weaker than $\omega^{-2}$. Such deviations can be described using a model with the distribution of values $\tau_d$ (or $E_a$) [32]. In this case, the dipole-dipole contribution to the spin-lattice relaxation rate is calculated as

$$T_{1d}^{-1} = \int T_{1d}^{-1}(E_a) G(E_a) dE_a, \tag{3}$$

where $G(E_a)$ is the normalized distribution of values $E_a$, and $T_{1d}^{-1}(E_a)$ is determined by the equations (1) and (2). We used the Gaussian form of the distribution function $G(E_a)$ to parameterize the data near the relaxation rate maximum. The parameters of our model are $M_{2\mathrm{HH}}$, $M_{2\mathrm{HCo}}$, $\tau_{d0}$, the average activation energy $(\overline{E_a})$ and the distribution dispersion $\Delta E_a$. These parameters were varied to find the best approximation of $T_{1d}^{-1}(T)$ data simultaneously at three resonance frequencies. The results of this approximation are shown by solid lines in Figure 4; the corresponding parameter values: $M_{2\mathrm{HH}} = 1.98(2) \cdot 10^9\,\mathrm{s}^{-2}$, $M_{2\mathrm{HCo}} = 2.3(2) \cdot 10^8\,\mathrm{s}^{-2}$, $\tau_{d0} = 3.1(2) \cdot 10^{-12}\,\mathrm{s}$, $\overline{E_a} = 60(3)\,\mathrm{meV}$, $\Delta E_a = 22(2)\,\mathrm{meV}$.

As already mentioned, in Figure 3 the relaxation rate maximum is observed at a frequency of 14.5 MHz at high temperature, in addition to the $T_1^{-1}$ peak at low temperature. Figure 5 shows the dependence of $T_{1d}^{-1}$ on the inverse temperature for $\mathrm{TiSe_2}\big(\mathrm{Co}(\pi-\mathrm{C_5H_5})_2\big)_{1/4}$ in the region of the high-temperature relaxation rate peak at a frequency of 14.5 MHz.

If we approximate $T_{1d}^{-1}(T)$ for this peak with the model described above, we obtain the following parameters for the reorientational motion of cobaltocene molecules: $M_{2\mathrm{HH}} = 2.96(2) \cdot 10^8\,\mathrm{s}^{-2}$, $M_{2\mathrm{HCo}} = 4.06(3) \cdot 10^7\,\mathrm{s}^{-2}$, $\tau_{d0}$=7.3(3) $\cdot\, 10^{-12}$ s, $\overline{E_a}$=155(2) meV, $\Delta E_a = 35(2)$ meV. It should be taken into account that this result is only an estimate, since the range of variation in the relaxation rate is very small and the approximation is carried out at a single resonant frequency. Thus, the analysis of experimental data on the proton spin-lattice relaxation rate for cobaltocene intercalated in titanium diselenide has demonstrated the existence of at least two types of reorientations of cobaltocene molecules (presumably around the axes of symmetry of the fifth and second order), and also allowed to estimate the motional parameters of these molecules.

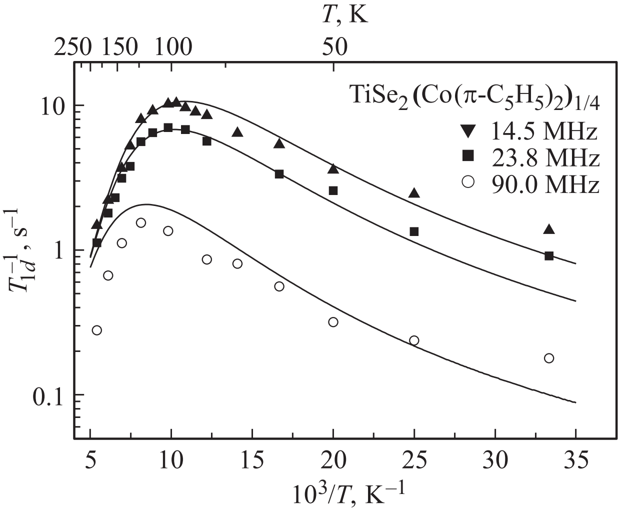

**Figure 4.** Dependence of the dipole contribution $T_{1d}^{-1}$ at frequencies 90, 23.8 and 14.5 MHz on the inverse temperature in $\mathrm{TiSe_2}\big(\mathrm{Co}(\pi-\mathrm{C_5H})5)_2\big)_{1/4}$. Solid lines show the results of modeling of this dependence within the framework of the standard model [31] with the distribution of activation energies.

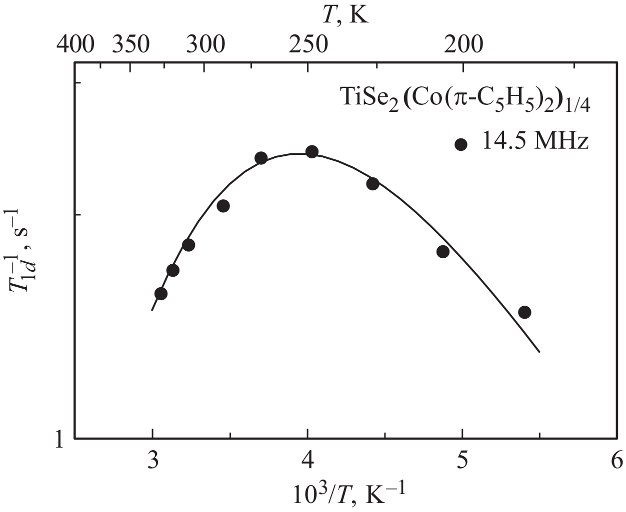

**Figure 5.** Dependence of the dipole contribution $T_{1d}^{-1}$ (on a logarithmic scale) at a frequency of 14.5 MHz on the inverse temperature in $\mathrm{TiSe_2}\big(\mathrm{Co}(\pi-\mathrm{C_5H_5})_2\big)_{1/4}$. The solid line shows the result of the approximation of this dependence within the framework of the standard model with the distribution of activation energies.

Figure 6 shows $^1$H NMR spectra in the temperature range of 5−80 K for $\mathrm{TiSe_2}\big(\mathrm{Co}(\pi-\mathrm{C_5H_5})_2\big)_{1/4}$. It should be noted that $^1$H NMR line significantly narrows in this low-temperature range with the increase of the temperature. This narrowing may be attributed to partial averaging of the dipole-dipole interactions of $^1$H nuclei due to the motion of cobaltocene molecules.

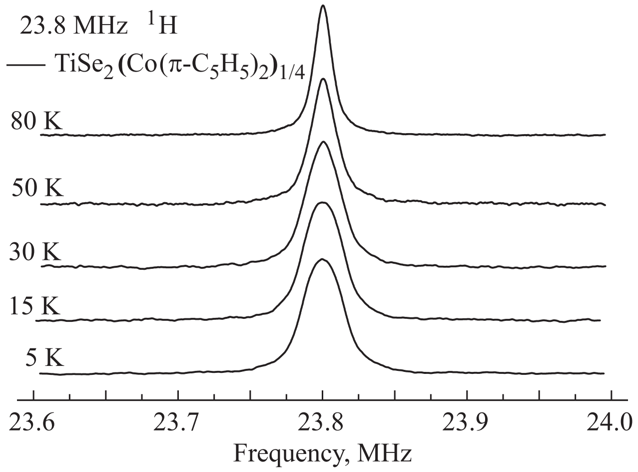

**Figure 6.** Evolution of the shape of $^1$H NMR line, measured at a frequency of 23.8 MHz, for $TiSe_2(Co(\pi-C_5H_5)_2)_{1/4}$.

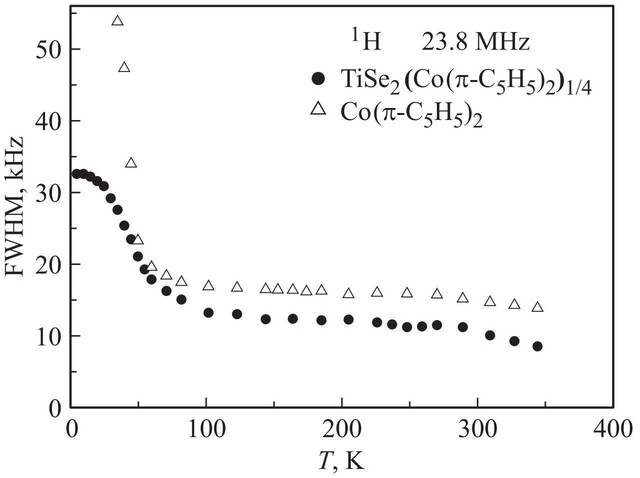

**Figure 7.** Temperature dependences of full width at half maximum (FWHM) of $^1$H NMR spectra measured at a frequency of 23.8 MHz for $TiSe_2(Co(\pi-C_5H_5)_2)_{1/4}$ and for molecular cobaltocene $Co(\pi-C_5H_5)_2$.

The change of line width as a function of temperature for this compound is shown in Figure 7.

Several regions of line width variation depending on temperature can be distinguished for cobaltocene intercalated in $TiSe_2$. The line width practically does not change in the range of 5–15 K and is equal to 32.6 kHz. This value can be considered as the dipole line width in a „rigid" lattice. Gradual narrowing of line to 13 kHz at 100 K, turning into a plateau to about 200 K is observed with a further increase of temperature. The existence of such a plateau is a characteristic feature of the local motion of H atoms. Indeed, the reorientational (local) motion leads only to a partial averaging of dipole-dipole interactions, in contrast to the long-range diffusion. It should be noted that a significant narrowing of the line due to motion should be observed when the jump rate $\tau_d^{-1}$ becomes comparable to the width of the line in a „rigid" lattice. The „step" on the temperature dependence of the line width should be shifted towards low temperatures with respect to the spin-lattice relaxation rate maximum for the same motion process, since the dipole width in a „rigid" lattice is several orders of magnitude smaller than the resonance frequency $\omega$. Therefore, the „step" in Figure 7 in the temperature range of about 50 K can be ascribed to the rapid reorientational process responsible for the $T_{1d}^{-1}(T)$ maximum near 100 K. Similarly, a slight narrowing of the line above 200 K (Figure 7) can be ascribed to the reorientational process responsible for the relaxation rate peak near room temperature (Figure 5). An additional narrowing of the line above 300 K (Figure 7) may indicate the excitation of another type of motion (for example, diffusion of cobaltocene molecules) on a frequency scale of the order of $10^5\,s^{-1}$. The nature of this motion could be clarified by measurements at higher temperatures; however, we did not perform measurements at temperatures exceeding 360 K to preserve the stability of the intercalated sample.

Our $^1$H NMR line width data are similar to the results obtained for cobaltocene intercalated in tantalum disulfide $TaS_2$ in Ref. [22]. Two types of reorientational motion of cobaltocene molecules were also observed in this study, corresponding to rotations around symmetry axes of the fifth order (fast process) and the second order (slow process). A model of the location of cobaltocene molecules in the interlayer space with fifth-order symmetry axes parallel to the dichalcogenide layers was also proposed in Ref. [22]. It should be noted, however, that such an orientation is not the only possible one, since the ratio of the height of the model cylinder describing the cobaltocene molecule to its diameter is close to unity (6.96 and 6.76 Å respectively [18]). Two orientations of $Co(\pi-C_5H_5)_2$ molecules with the fifth-order symmetry axes parallel and perpendicular to the layers of dichalcogenide are possible for cobaltocene intercalated in $TaS_2$ [23,26].

Generally, the information on the geometric aspects of reorientational motion can be obtained from quasi-elastic neutron scattering (QENS) experiments. There are no such experiments for metallocenes intercalated into layered dichalcogenides; measurements by the QENS method were carried out only for some molecular metallocenes — ferrocene, nickelocene and ruthenocene [33,34]. It should be noted that due to the limited energy-transfer resolution for the existing neutron spectrometers, the QENS method allows to study only fast reorientational motion (with jump rates exceeding $10^9\,s^{-1}$). QENS studies have shown that $C_5H_5$ rings perform reorientational jumps with the angles of $2\pi/5$ or $2\pi/10$ around the fifth-order symmetry axis in the ferrocene, nickelocene, and ruthenocene [33,34]. The activation energy for reorientational motion in ferrocene, found by this method in the temperature range above 164 K, is 46 meV [33]. The activation energy for reorientations around the fifth-order axis in the nickelocene determined from the QENS experiments in the temperature range of

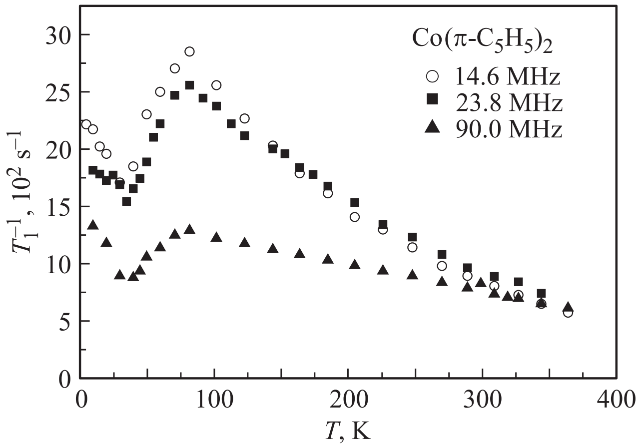

**Figure 8.** Temperature dependences of the spin-lattice relaxation rate of $^1$H in $Co(\pi-C_5H_5)_2$ at three resonance frequencies.

155−300 K, is 65 meV [34]. These values of activation energies are of the same order of magnitude as the average activation energy (60 meV) that we found for the fast reorientation process in $TiSe_2(Co(\pi-C_5H_5)_2)_{1/4}$.

We have also measured $^1$H NMR parameters in molecular cobaltocene, to compare with the results obtained for cobaltocene intercalated in $TiSe_2$. The results of measurements of the $^1$H spin-lattice relaxation rate, $T_1^{-1}$, in $Co(\pi-C_5H_5)_2$ as functions of temperature are shown in Figure 8.

The comparison with the data shown in Figure 3 shows that the maximum relaxation rates for molecular cobaltocene are 2−3 orders of magnitude higher than the relaxation rates in the intercalated sample. The observed maximum of $T_1^{-1}$ in molecular cobaltocene cannot be related to the modulation of the dipole-dipole interaction between nuclear spins. Indeed, the calculation of the second moment of $^1$H NMR line for a static cobaltocene molecule yields $1.65 \cdot 10^9\,s^{-2}$, which results in a maximum value of the spin-lattice relaxation rate equal to $12.8\,s^{-1}$ at a frequency of 23.8 MHz, according to formula (1) for the dipole mechanism. The experimental maximum value of $T_1^{-1}$ at this frequency for molecular cobaltocene exceeds $2500\,s^{-1}$. This comparison shows that the dominant mechanism of spin-lattice relaxation in molecular cobaltocene is associated with fluctuations in the electron magnetic moment localized on Co. Measurements of the proton spin-lattice relaxation rate in this compound do not allow obtaining information on the molecular motion. On the other hand, when cobaltocene is intercalated in $TiSe_2$, its ionization takes place, leading to suppression of the localized electron magnetic moment.

It should be noted that the temperature of the $T_1^{-1}$ maximum in molecular cobaltocene approximately coincides with the temperature of the structural phase transition in this compound [8,9] and does not depend on the resonance frequency. These facts may serve as additional confirmation that this maximum is not related to molecular motion. An additional increase of the spin-lattice relaxation rate below 35 K (Figure 8) may be attributed to the antiferromagnetic ordering [7]. A very large width of $^1$H NMR spectrum in molecular cobaltocene is also consistent with the magnetic ordering at low temperatures. The spectrum width at half height exceeds 100 kHz at $T = 5\,K$; such a width cannot be explained solely by dipole-dipole interactions between nuclear spins. Data on the $^1$H NMR line width in molecular cobaltocene in the temperature range above 30 K are included in Figure 7. As can be seen from this figure, the behavior of the line width in molecular cobaltocene at temperatures above 50 K resembles similar data for cobaltocene intercalated in $TiSe_2$, and may be associated with the reorientational motion of molecules.

## 4. Conclusion

Measurements of the $^1$H NMR parameters for cobaltocene intercalated into layered titanium diselenide have shown that the proton spin-lattice relaxation rate in this system is determined by fluctuations in the dipole-dipole interaction between nuclear spins that occur due to the reorientational motion of cobaltocene molecules. The existence of at least two types of reorientation motion of $Co(\pi-(C_5H_5)_2)$ molecules has been found. The faster reorientational process associated with rotations of $C_5H_5$ rings around the fifth-order symmetry axis is characterized by an activation energy of 60 meV. The reorientation rate reaches approximately $10^8\,s^{-1}$ for this process already at a temperature of 100 K. The slow process associated with the reorientations of cobaltocene molecules around the second-order symmetry axis is characterized by an activation energy of 155 meV; the reorientation rate for this process reaches $10^8\,s^{-1}$ near room temperature. The spin-lattice relaxation of protons in molecular cobaltocene is determined by fluctuations of the electronic local magnetic moment on cobalt, in contrast to cobaltocene intercalated in $TiSe_2$.

### Funding

The study was performed under the state assignment on the topic „Function“ No. 122021000035-6.

### Conflict of interest

The authors declare that they have no conflict of interest

## References

[1] J.D. Dunitz, L.E. Orgel. Nature **171**, *4342*, 121 (1953).
[2] M.Yu. Antipin, K.A. Lyssenko, R. Boese. J. Organometal. Chem. **508**, *1−2*, 259 (1996).
[3] W. Bünder, E. Weiss. J. Organometal. Chem. **92**, *1*, 65 (1975).
[4] R.D. Rogers, J.L. Atwood, D. Foust, M.D. Rausch. J. Crystal. Molecular Structure **11**, *5*, 183 (1981).
[5] A. Haaland. Acc. Chem. Res. **12**, *11*, 415 (1979).

[6] T.B. Woldeamanuale. J. Phys. Chem. Biophys. **6**, *5*, 1000226 (2016).

[7] J.H. Ammeter, J.D. Swalen. J. Chem. Phys. **57**, *2*, 678 (1972).

[8] I.B. Rabinovich, V.P. Nistratov, M.S. Sheiman, G.V. Burchalova. J. Chem. Thermodyn. **10**, *6*, 523 (1978).

[9] M.Yu. Antipin, R. Boese, N. Augart, G. Schmid. Struct. Chem. **4**, *2*, 91 (1993).

[10] M.B. Dines. Sci. *188*, *4194*, 1210 (1975).

[11] M. Rajapakse, B. Karki, U.O. Abu, S. Pishgar, M.R.K. Musa, S.M.S. Riyadh, M. Yu, G. Sumanasekera, J.B. Jasinski. npj 2D Mater. Appl. **5**, *1*, 30 (2021).

[12] D.-Y. Kuo, P.S. Rice, S. Raugei, B.M. Cossairt. J. Phys. Chem. C **126**, *32*, 13994 (2022).

[13] D. O'Hare, J.S.O. Evans. Comments. Inorg. Chem. **14**, *2–3*, 155 (1993).

[14] R.H. Friend, A.D. Yoffe. Adv. Phys. **36**, *1*, 1 (1987).

[15] D. O'Hare, J.S.O. Evans, P.J. Wiseman, K. Prout. Angew. Chem. Int. Ed. Engl. **30**, *9*, 1156 (1991).

[16] D. O'Hare, W. Jaegermann, D.L. Williamson, F.S. Ohuchi, B.A. Parkinson. Inorg. Chem. **27**, *9*, 1537 (1988).

[17] L. Hernán, J. Morales, L. Sánchez, J.L. Tirado, J.P. Espinós, A.R. González Elipe. Chem. Mater. **7**, *8*, 1576 (1995).

[18] H.-V. Wong, J.S.O. Evans, S. Barlow, S.J. Mason, D. O'Hare. Inorg. Chem. **33**, *24*, 5515 (1994).

[19] A. Ibarz, E. Ruiz, S. Alvarez. J. Chem. Soc., Dalton Trans. **9**, 1463 (2000).

[20] A. Ibarz, E. Ruiz, S. Alvarez. J. Mater. Chem. **8**, *8*, 1893 (1998).

[21] A.V. Skripov, A.V. Soloninin, O.A. Babanova, R.V. Skoryunov. Molecules **25**, *12*, 2940 (2020).

[22] B.G. Silbernagel. Chem. Phys. Lett. **34**, *2*, 298 (1975).

[23] S.J. Heyes, N.J. Clayden, C.M. Dobson, M.L.H. Green, P.J. Wiseman. J. Chem. Soc., Chem. Commun. **20**, 1560 (1987).

[24] C. Grey, J.S.O. Evans, D. O'Hare, S.J. Heyes. J. Chem. Soc., Chem. Commun. **19**, 1380 (1991).

[25] S.J. Mason, S.J. Heyes, D. O'Hare. J. Chem. Soc., Chem. Commun. **16**, 1657 (1995).

[26] J.S.O. Evans, D. O'Hare. Chem. Mater. **7**, *9*, 1668 (1995).

[27] O.N. Suvorova, G.A. Domrachev, E.A. Shchupak, G.S. Kudryavtseva, G.K. Fukin, S.Yu. Ketkov, I.L. Vasilevskaya. Rus. Chem. Bull., Intern. Ed. **56**, *5*, 910 (2007).

[28] A.N. Titov, O.N. Suvorova, S.Yu. Ketkov, S.G. Titova, A.I. Merentsov. Phys. Solid State **48**, *8*, 1466 (2006).

[29] S.V. Ovsyannikov, V.V. Shchennikov, A.N. Titov, Y. Uwatoko. Physica Status Solidi (b) **244**, *1*, 174 (2007).

[30] A.N. Titov, N.A. Shaidarova, S.V. Ovsyannikov, V.V. Shchennikov, G.S. Kudryavtseva, S.Yu. Ketkov. Phys. Solid State **50**, *5*, 941 (2008).

[31] A. Abragam. The Principles of Nuclear Magnetism. Oxford University Press (1961).

[32] J.T. Markert, E.J. Cotts, R.M. Cotts. Phys. Rev. B **37**, *11*, 6446 (1988).

[33] A.B. Gardner, J. Howard, T.C. Waddington, R.M. Richardson, J. Tomkinson. Chem. Phys. **57**, *3*, 453 (1981).

[34] C. Sourisseau, G. Lucazeau, A.J. Dianoux, C. Poinsignon. Mol. Phys. **48**, *2*, 367 (1983).

*Translated by A.Akhtyamov*